Hyperfine fields at impurities in ferromagnetic metals

S. Estreicher
Institut für Theoretische Physik der Universität, Zürich, CH-8001 Zürich, Switzerland

P. F. Meier
Physik-Institut der Universität Zürich, CH-8001 Zürich, Switzerland

(Received 11 March 1981)

A model has been developed which describes the hyperfine field at nonmagnetic impurities in ferromagnetic metallic hosts as arising from conduction-electron polarization. The problem is approached by considering the effect of both the screened electrostatic potential of the impurity and a spin-dependent potential arising from the exchange scattering of the conduction electrons at the localized magnetic moments of the host lattice. The influence of zero-point motion and thermal vibrations is explicitly taken into account. The model is applied to study the spin density at muons in Gd, Dy, Ni, Fe, and Co, and the predictions of the model are compared with experiment. The effect of various physical mechanisms on the temperature, pressure, and site dependence of the hyperfine field is discussed in detail.

I. INTRODUCTION

In the last few years the muon spin rotation (μSR) technique has been widely used to investigate internal fields in magnetically ordered materials.[1,2] Once thermalized in condensed matter, the positive muon behaves as if it were a light proton ($m_p/m_\mu \approx 9$). The precession frequency which is observed by detecting the time-dependent angular correlation pattern of the decay positron gives a direct quantitative measure of the local magnetic field B_μ at the site of the muon. By considering the contributions of the Lorentz field and the residual dipolar field to B_μ,[3] the site of the muon and the contact hyperfine field can be determined.

The hyperfine fields thus observed in various ferromagnetic metals are all negative, i.e., the local magnetization density at the μ^+ is in a direction opposite to the average magnetization density. Such a negative value is in agreement with other experiments at dilute nonmagnetic impurities in ferromagnetic metals which generally show hyperfine fields which are negative for small impurity valence Z and positive for large Z. This dependence was first explained by Daniel and Friedel.[4] They proposed a model which assumes a homogeneous free-electron gas with a positive spin polarization. Simulating the electrostatic potential of the impurity by a square well, the depth of which depends on Z, the spin density at the impurity is then calculated. Although most applications of this model have dealt with substitutional impurities, it is equally applicable to interstitials. Another model for hyperfine fields was proposed by Blandin and Campbell,[5] who, instead of assuming an *a priori* spin-polarized electron gas, considered a Ruderman-Kittel-Kasuya-Yosida (RKKY)-type interaction between the localized moments of the host and the conduction electrons, giving rise to an inhomogeneous spin polarization. Other models have been proposed by Jena and Geldart,[6] who explained qualitatively the behavior of hyperfine fields for a large number of Heusler alloys, and by Stearns,[7] who proposed a model based upon the volume misfit between the impurity and host atoms.

The results of the μSR experiments in ferromagnetic metals have provoked new theoretical efforts to explain the measured hyperfine fields. Microscopic calculations of spin densities at muons in Ni have recently been presented by several authors using different approaches such as separate treatment of s and d electrons,[8] a molecular cluster calculation,[9] a Korringa-Kohn-Rostoker (KKR) formalism,[10,11] or a supercell band-structure method.[12] While giving values of $B_{\rm hf}(T=0)$ at the μ^+ in Ni in good agreement with experiment, due to computational complexity these methods are inconvenient to study the influence of different physical effects on the spin density. Effects such as zero-point motion of the muon, lattice relaxation, and lattice expansion are best studied in the framework of a

phenomenological model.

The first attempts[13] concentrated on the spin-density enhancement at a μ^+ in a homogeneously polarized electron gas with a polarization determined by the background density measured with neutrons. It has been pointed out,[14] however, that it is not adequate to base a model on a homogeneously polarized electron gas. The hyperfine field is a nonlocal quantity and the use of a local density approximation is incorrect.

In the present paper a model is developed which describes the hyperfine field as arising from conduction electron polarization. It is an extension of previous works[15–17] devoted to the study of spin densities at positive muons. It contains other models as special cases (Daniel-Friedel[4] and Blandin-Campbell[5]), and includes the main perturbations created by the presence of the muon in the lattice. These perturbations seem to be essential in explaining the experimental data. Similar models have recently been proposed,[18,19] which also stress the nonlocal character of the hyperfine field at the impurity.

Since the model is based on a spin-dependent potential arising from the exchange scattering of conduction electrons at localized magnetic moments, it treats the exchange mechanism in an approximate manner. Therefore, it does not allow precise predictions of the absolute numerical values of the hyperfine fields at impurities. However, the present model has the merit of providing a physically transparent picture and allows one to study in some detail how the hyperfine fields are influenced by various physical mechanisms. In particular, the modifications due to the zero-point motion of the impurity (which is large in the case of a light impurity as the μ^+) and the effects of thermal vibrations of the lattice ions and of thermal expansion are investigated. For technical reasons these physical effects are usually neglected in first-principle calculations.

The outline of the paper is as follows. In Sec. II the model is developed for an arbitrary nonmagnetic impurity in a ferromagnetic metal. Its relation to other models[4,5,19] is discussed. Zero-point motion and thermal lattice vibrations are taken into account in a way similar to the discussion of the temperature dependence of the electric field gradients at impurities in metals.[20,21] The theory is presented for a general impurity but has been applied so far only to muons or protons.

The model parameters are discussed in Sec. III, and the results of the model applied to the pure host lattice are described in conjunction with the data from polarized neutron scattering. Section IV is devoted to the dependence of the hyperfine fields on vibrations of the muon and lattice ions. Two typical examples (Gd and Ni) are discussed for various values of the model parameters as well as for different sites of the muon. The results are compared with the experimental data which are summarized in Table I.

In order to provide some physical insight into the numerical results of Sec. IV, we discuss the dependence of spin densities on vibrations in the framework of a modified RKKY model in an Appendix. This simple model allows an analytical expansion of the spin density in terms of a vibration parameter which shows that the hyperfine fields depend crucially on the distance between the impurity and the first neighboring ions. These structural effects are used to discuss in detail the results of the full model presented in Sec. IV.

The model allows one to consider changes in the lattice parameters and vibration amplitudes in a straightforward way. Thus, in Secs. V and VI the temperature, pressure, and site dependencies are investigated. The experimental functions $B_{\rm hf}(T)$ do not scale with the temperature-dependent saturation magnetization $M_s(T)$ of the host. The measured deviation $D(T)$, defined by

$$D(T)=\frac{B_{\rm hf}(T)}{B_{\rm hf}(0)}-\frac{M_s(T)}{M_s(0)}\ , \tag{1}$$

keeps the same sign for $T<T_c$, and it can be positive or negative (see Table I). In the framework of the present model this behavior can be partially reproduced.

Furthermore, it is shown that the discontinuity of the hyperfine field at the structural phase transition in Co can be qualitatively understood with the

TABLE I. Compilation of the experimentally determined zero-temperature hyperfine field $B_{\rm hf}(0)$, the determined muon site, and the deviation $D(T)$ of the normalized hyperfine field $B_{\rm hf}(T)$ from the bulk magnetization [Eq. (1)]. The table is from Ref. 1.

Host	$B_{\rm hf}(0)$ (kG)	$D(T)$	Site
Gd	$-6.9\ \pm0.2$	<0	octahedral
Dy	-0.7 or -25.0	?	octahedral (?)
Ni	-0.71 ± 0.01	>0	octahedral (?)
Fe	$-11.1\ \pm0.2$	<0	tetrahedral (?)
Co	$-6.1\ \pm0.2$	<0	octahedral

help of the vibration dependence of B_{hf} in both phases. The main conclusions of this study are summarized in Sec. VII.

II. DESCRIPTION OF THE MODEL

We consider a ferromagnetic host lattice with a single nonmagnetic impurity located at the origin, which may be a substitutional or an interstitial site. The screened electrostatic potential produced by the impurity gives rise to a distortion of the wave functions of the conduction electrons, which are treated as an interacting electron gas. The magnetic moments $\vec{S}$ localized at the lattice sites $\vec{R}_{\vec{m}}$ of the ferromagnetic host interact with the spin $\vec{s}$ of the conduction electrons through an effective s-d or s-f exchange interaction

$$H_{ex}=-2J_{ex}\vec{s}\cdot\vec{S}\Omega\sum_{\vec{m}}\delta(\vec{r}-\vec{R}_{\vec{m}}) \tag{2}$$

with interaction energy J_{ex}. Ω denotes the atomic volume. The sum extends over all occupied lattice sites $\vec{R}_{\vec{m}}$. Following Blandin and Campbell,[5] we simulate this interaction by the spin-dependent potential

$$W_\sigma(\vec{r})=-\sigma J_T\Omega\sum_{\vec{m}}\delta(\vec{r}-\vec{R}_{\vec{m}})\ . \tag{3}$$

$\sigma=\pm1$ according to the spin projection of the conduction electrons. The effective exchange energy

$$J_T=J_{ex}\langle S_z\rangle=J_0\frac{M_s(T)}{M_s(0)} \tag{4}$$

is temperature dependent since the average localized moment $\langle S_z\rangle$ is supposed to follow the saturation magnetization $M_s(T)$. Since we are interested in the charge and spin densities close to the impurity only, the model is further simplified by taking a spherical average of $W_\sigma(\vec{r})$:

$$W_\sigma(r)=\frac{1}{4\pi}\int d(\cos\theta)d\phi\, W_\sigma(\vec{r})\ . \tag{5}$$

This approximation is analogous to the spherical solid model,[22] where the electrostatic lattice potential is approximated by a spherical average of the ion pseudopotentials. In our case the pseudopotentials of the lattice ions are ignored, and only the influence on the spin dependence of the conduction electrons is considered.

For large r values, $W_\sigma(r)$ can be replaced by its average

$$\overline{W}_\sigma=-\sigma J_T\ . \tag{6}$$

This constant part of the potential gives rise to a rigid band splitting described by the Fermi wave vectors k_F^σ:

$$(k_F^\sigma)^2-k_F^2=2\overline{W}_\sigma=-2\sigma J_T\ . \tag{7}$$

In a linear approximation, the corresponding mean polarization of the itinerant electrons is given by

$$\frac{\Delta n_0}{n_0}=\frac{3}{2}\frac{J_T}{E_F} \tag{8}$$

where $n_0=k_F^3/(3\pi^2)$ is the density, and $E_F=\frac{1}{2}k_F^2$ the Fermi energy of the homogeneous electron gas. From Eqs. (3), (5), and (7), the inhomogeneous magnetic potential is found to be

$$\Delta W_\sigma(r)=W_\sigma(r)-\overline{W}_\sigma=-\sigma J_T\left[\Omega\sum_s\frac{z_s}{4\pi R_s^2}\delta(r-R_s)-1\right]\ . \tag{9}$$

Now the sum extends over all shells s at distance R_s from the impurity, and z_s denotes the number of ions on shell s.

As has been discussed earlier,[16] this model contains the model of Daniel and Friedel[4] as well as that of Blandin and Campbell[5] as limiting cases: By neglecting ΔW_σ altogether and approximating the charge screening potential by a square well, one recovers precisely the Daniel-Friedel model which has been proposed to explain the hyperfine field systematics observed at impurities with different valences in ferromagnets. On the other hand, by restricting the sum over s to a few neighboring shells around the impurity, one obtains the model of Blandin and Campbell. In this case, the constant part $\overline{W}_\sigma$ must be set equal to zero since there is no band splitting of the electron gas.

The spin-dependent potential $W_\sigma(\vec{r})$ introduced in Eq. (3) assumes fixed sites for the ions (at $\vec{r}=\vec{R}_{\vec{m}}$) and for the nonmagnetic impurity (at $\vec{r}=\vec{0}$). Actually this potential depends on the instantaneous positions and should be replaced by

$$W_\sigma(\vec{r},t)=-\sigma J_T\Omega\sum_{\vec{m}}\delta(\vec{r}-\vec{R}_{\vec{m}}-\vec{u}_{\vec{m}}(t)+\vec{u}_\mu(t))\ , \tag{10}$$

where $\vec{u}_{\vec{m}}(t)$ is the instantaneous displacement of the lattice ion $\vec{m}$ from its average position $\vec{R}_{\vec{m}}$ and $\vec{u}_\mu(t)$ that of the muon probe. By requiring that the mean elongations vanish,

$$\langle\vec{u}_{\vec{m}}(t)\rangle=0\ , \tag{11}$$

all effects due to lattice expansion are shifted into the quantities $\vec{R}_{\vec{m}}$ which thus become temperature dependent.

Since measurements of the hyperfine field act on a time scale much larger than that for thermal vibrations, the potential (10) may be averaged over phonon fluctuations:

$$W_\sigma(\vec{r}) = \langle W_\sigma(\vec{r},t) \rangle \ . \tag{12}$$

Writing the δ function in Eq. (10) as an integral, one obtains

$$W_\sigma(\vec{r}) = -\sigma J_T \Omega \sum_{\vec{m}} \int \frac{d^3q}{(2\pi)^3} e^{i\vec{q}\cdot(\vec{r}-\vec{R}_{\vec{m}})} \times \langle e^{-i\vec{q}\cdot[\vec{u}_{\vec{m}}(t)-\vec{u}_\mu(t)]} \rangle \ . \tag{13}$$

The average over the exponential can be treated by the cumulant method, which is applicable even in the case of strongly anharmonic vibrations. In the present context however, it is sufficient to consider the simplest harmonic case and to assume that the motion of the ions and of the impurity are uncorrelated. Using the Debye-Waller approximation, one may then approximate the expectation value by

$$\langle e^{-i\vec{q}\cdot[\vec{u}_{\vec{m}}(t)-\vec{u}_\mu(t)]} \rangle \cong e^{-q^2(\langle u_m^2 \rangle + \langle u_\mu^2 \rangle)/6} \ , \tag{14}$$

where it has been assumed that $\langle \vec{u}_\mu \rangle = 0$.

Taking the spherical average of $W_\sigma(\vec{r})$, we get for the magnetic part of the potential

$$W_\sigma(r) = -\frac{\sigma J_T \Omega}{4\pi} \sum_s \frac{z_s}{rR_s} \frac{1}{\sqrt{\pi} a \eta} e^{-(r-R_s)^2/a^2\eta^2} \ . \tag{15}$$

The dimensionless parameter η defined by

$$\eta^2 = \frac{2}{3} \frac{\langle u_m^2 \rangle + \langle u_\mu^2 \rangle}{a^2} \tag{16}$$

is a measure for the combined mean-square elongations of the nonmagnetic impurity and of the host ions in units of the lattice constant a.

The inhomogeneous magnetic potential

$$\Delta W_\sigma(r) = W_\sigma(r) - \overline{W}_\sigma \tag{17}$$

is rather long ranged and has an oscillatory behavior (Fig. 1). The vibrations have the effect of smoothing out the δ functions of the rigid lattice.

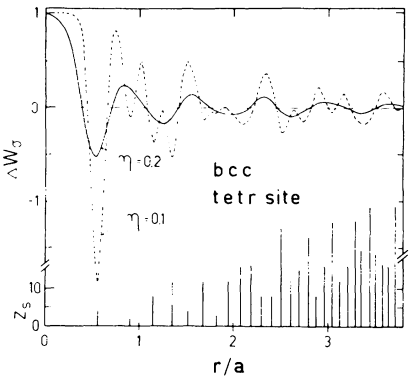

FIG. 1. Inhomogeneous magnetic potential $\Delta W_\sigma(r)$ for $\sigma = +1$ [see Eqs. (15) and (17)], in units of J_T, versus the distance from the tetrahedral interstitial site in the bcc lattice. For $\eta = 0$, $\Delta W_\sigma(r)$ is a sum of δ functions [see Eq. (9)]. For $\eta \neq 0$, it becomes a sum of Gaussians with widths which increase with η. In the lower part of the figure, the number z_s of ions on shell s is shown.

It should be mentioned that the localized exchange interaction (2) is an idealization; the corresponding δ functions should be replaced by Gauss functions with a width given by the spread of the wave functions responsible for the localized magnetic moment. This effect can easily be incorporated into the model by adding to the right-hand side of Eq. (16) the relative mean-square spread, leading to an enhancement of the value of the parameter η.

Given the magnetic potential and the pure Coulomb attraction of the charge of the nonmagnetic impurity ($-Z/r$), the spin density of the electrons can be calculated in the framework of the self-consistent density-functional method. This technique has been applied[18] to the investigation of the hyperfine field systematics for impurities with various outer electron configurations in Ni. Light impurities in Gd and Dy have recently been treated with the density-functional method by Manninen and Nieminen.[19] The excessive numerical work involved in these calculations, however, forces one to cut off the potential after the first few shells.

In the present work we therefore choose to approximate the effective electrostatic potential by a one-parameter potential

$$V_\lambda(r) = -\frac{2\lambda}{e^{2\lambda r} - 1} \ , \tag{18}$$

where λ is determined from the Friedel sum rule.

It has been shown[23] that the electron density at a muon in a homogeneous electron gas calculated with $V_\lambda(r)$ differs from that calculated in the self-

consistent density-functional formalism by at most 10% over the entire metallic range. Significant discrepancies occur only for large r values. The physical reason for this is the fact that close to the impurity the potential is always dominated by the Coulomb part. The specific form (18) was chosen since it allows an analytic solution of all s-wave properties.[24] Another choice for $V_\lambda(r)$ (e.g., a Yukawa-type potential) would not significantly affect the resulting spin density.

The problem is now reduced to calculating the electron wave functions in each band σ for the spherical symmetric potential

$$\Phi_{\sigma,\lambda}(r)=V_\lambda(r)+W_\sigma(r)-\overline{W}_\sigma \ , \tag{19}$$

which is represented in Fig. 2. To achieve a reasonable independence from the cutoff radius, a very large number of lattice points (typically one thousand) must be taken into account.

Denoting the enhancement factor[24] for the wave functions with wave vector $\vec{k}$ by $E_\sigma(\vec{k})$, the spin density at the origin resulting from the potential $\Phi_{\sigma,\lambda}(r)$ can be written

$$\Delta n(0)=\frac{1}{2\pi^2}\left[\int_0^{k_F^+} dk\, k^2 E_+(k) - \int_0^{k_F^-} dk\, k^2 E_-(k)\right]+\Delta n(0)_b \tag{20}$$

where $\Delta n(0)_b$ denotes the spin density originating from bound states. The contributions of the scattering and bound states to the total spin density, shown for a typical case in Fig. 3, involve cancellation of large individual contributions, so that high numerical accuracy is required for a reliable net spin density. It is of interest to note that the contribution from the scattering states alone results in a positive spin density. The bound state, on the other hand, gives rise to a negative polarization. This behavior is common to all cases investigated in this paper and indicates that the model simulates rather well some of the basic features found in much more fundamental calculations. (See, e.g., the discussion of Kanamori *et al.*[11] of the contributions of band and bonding states to the total spin density at the μ^+ in Ni.)

III. DISCUSSION OF THE MODEL PARAMETERS AND THE UNPERTURBED SPIN DENSITY

The model contains two essential parameters: J_0, the effective exchange interaction at 0 K, and η, a measure of the vibrations. The former quantity is independent of the presence of the impurity, and its value can, in principle, be estimated from experiment. Dividing the spin density in a ferromagnetic metal into one contribution from localized moments and another from itinerant electrons

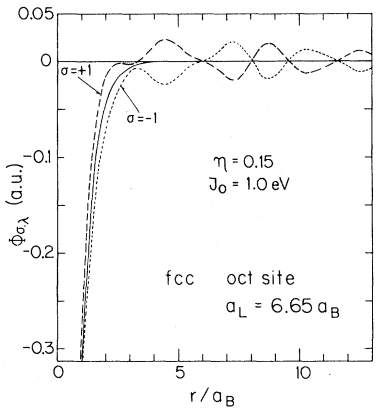

FIG. 2. Plot of the total potential $\Phi_{\sigma,\lambda}(r)$ in atomic units [Eq. (19)]. The solid line is the charge screening potential alone, $V_\lambda(r)$ [Eq. (18)], with $\lambda=0.95$. The dashed and dotted lines include the magnetic potential for both spin directions. The impurity is at the origin (octahedral interstitial site in the fcc lattice).

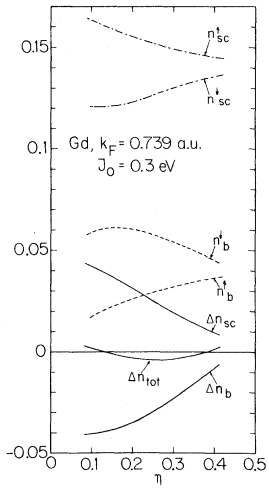

FIG. 3. Contributions to the spin density in atomic units versus η, at a positive muon localized at the octahedral interstitial site in Gd. $\Delta n_{\rm tot}=\Delta n_{\rm sc}+\Delta n_b=n^{\uparrow}_{\rm sc}-n^{\downarrow}_{\rm sc}+n^{\uparrow}_b-n^{\downarrow}_b$, contains the scattering and bound states contributions. For higher values of η, both $\Delta n_{\rm sc}$ and Δn_b may cross the 0 axis.

is a reasonable approximation in the case of rare-earth metals. The atomic f-electron contribution for Gd (Dy) is $7\mu_B$ ($10\mu_B$). From the measured magnetization of $7.55\mu_B$ ($10.2\mu_B$) per atom, a mean itinerant spin density of 0.0025 a.u. (0.000 94 a.u.) is obtained. Equations (4) and (8) then give $J_{ex}=0.24$ eV (0.063 eV), i.e., $J_0=0.83$ eV (0.31 eV).

For transition metals, the use of a localized exchange interaction is somewhat artificial. However, since the long-range potential obtained mimics the spatially inhomogeneous spin polarization of the host, it contains some of the essential physics of an impurity in a ferromagnet.

By leaving the value of J_0 as a parameter, we focus not on the values of the calculated hyperfine fields, but rather on the influence of different mechanisms on the spin density. In general we expect J_0 to be smaller for transition metals than for Gd.

An estimate for J_0 may be obtained by calculating the magnetization at an interstitial site in the absence of a muon. The resulting unperturbed spin densities are given in Table II for $J_0=0.9$ eV (Gd) or 0.3 eV (Ni,Fe,Co). It is remarkable that the model calculations lead to a negative magnetization at all interstitial sites although the mean magnetization of the itinerant electrons is assumed positive. This clearly shows the nonlocal character of the spin polarization, as pointed out earlier.[14] The calculated magnetization may be compared with the value obtained from polarized neutron scattering experiments in Gd,[25] Ni,[26] Fe,[27] and Co.[28] In these experiments, the magnetization distribution is determined as a Fourier series expansion of the magnetic Bragg reflection amplitudes. The Fourier series method gives accurate results for the distribution in the region close to the lattice site, but it converges too slowly to give precise information about the interstitial regions since only a finite number of Bragg reflections (about 30) could be measured. By averaging the magnetization over regions of space, the effects due to finite resolution can be minimized. An alternate method for analyzing neutron scattering data is to fit the measured magnetic form factor to a free atom $3d$ spin form factor plus a constant term corresponding to a uniform contribution to the magnetization. The values of the magnetization given by both methods are compared to our calculations in Table II.

The model calculations give different values for the octahedral and tetrahedral interstitial sites in Ni but almost the same values for both sites in Fe. On the other hand, if analyzed by the first method, the neutron scattering data give a pronounced difference for the two sites in Fe, although with large error bars.

The other parameter of the model η was defined in Eq. (16). Its value is mainly given by the zero-point motion of the muon. Model calculations of the muon potential in Cu (Ref. 29) and in Ni (Ref. 30) in the vicinity of the octahedral site give values for $\langle u_\mu^2 \rangle^{1/2}$ of $1.3a_B$ and $0.9a_B$, respectively. These correspond to η values of about 0.2–0.3.

Another estimate may be obtained by calculating the radii ρ_{oct}, ρ_{tetr}, and ρ_{subst} of a sphere at the interstitial or substitutional sites which fits into the space left by touching spheres centered on the lattice sites. The corresponding η values are given in Table III. Since the ionic radius is always smaller

TABLE II. Unperturbed magnetization densities at interstitial sites. The model calculations are compared to the results obtained by neutron scattering data. The experimental results can be analyzed either by averaging the magnetization (method 1), or by fitting the magnetic form factor to the form factor of a free $3d$ atom (method 2).

	Magnetization (μ_B Å^{-3})		
		Experimental data	
	Theory	Method 1	Method 2
Gd, $J_0=0.9$ eV	−0.0192 (oct)	−0.037±0.004	
Ni, $J_0=0.3$ eV	−0.0087 (oct) −0.0025 (tet)	−0.0085	−0.0092
Fe, $J_0=0.3$ eV	−0.0077 (oct) −0.0076 (tet)	+0.0085±0.0068 (oct) −0.0136±0.0043 (tet)	−0.018
Co, $J_0=0.3$ eV	−0.0044 (oct)	−0.02	−0.025 ±0.006

than the touching sphere radius, we expect η to be generally larger than the values calculated. It is interesting to notice that the volume V_{oct} of the inscribed sphere at the octahedral site in a fcc lattice is larger by a factor of 6.2 than the volume V_{tetr} at the tetrahedral site. For a bcc lattice, one has $V_{tetr}/V_{oct}=6.7$, and for an hcp lattice with ideal c/a ratio $V_{oct}/V_{tetr}=6.3$. From the experimentally determined sites (see Table I) it thus seems that the preferred interstitial site of the muon corresponds to that where the maximum space is available.

As a function of temperature, the elongation $\langle u_\mu^2 \rangle^{1/2}$ is expected to increase slightly due to lattice expansion. This is taken into account by using the appropriate lattice constant in the calculation of potentials. The vibrations of the ions and their temperature dependence are known from measurements of the Debye-Waller factor.[31–33] The temperature dependence of η is shown in Fig. 4 for the particular value $\langle u_\mu^2 \rangle^{1/2}=0.775a_B$ for Gd, Ni, Fe, and Co. It should be noticed that the increase of the lattice constant a with temperature does not fully compensate the increase of $\langle u_m^2 \rangle^{1/2}$, so η is always a slightly increasing function of T.

IV. INFLUENCE OF VIBRATIONS

The model discussed in Sec. II has been applied to calculate the spin densities for a muon at various sites in different hosts. In this section two typical examples are discussed in detail: Gd and Ni.

The results for the octahedral site in Gd are shown in Fig. 5 where the spin density and the corresponding hyperfine fields are plotted as a function of η. It is seen that the spin density is extremely sensitive to small changes of η and is positive for both very small and large values of the elongation amplitudes. Since the actual values for η are expected to lie between 0.2 and 0.3, the model predicts negative hyperfine fields. Using the value $J_0=0.83$ eV, which is estimated from the excess magnetic moment of the conduction electrons (see Sec. III), the resulting hyperfine field is between -4.0 and -6.0 kG. This is in reasonable agreement with the experimental value -6.9 kG. A similar curve is obtained for Dy where, for $J_0=0.3$ eV, we obtain $-2.0\leq B_{hf}\leq -1.5$ kG. The result for Gd agrees rather well with the recent calculations of Manninen and Nieminen[19] who treated the charge screening in a fully self-

TABLE III. Maximum elongation of the vibration of the muon in the "touching spheres lattice" and corresponding values of η [Eq. (16)] calculated at the substitutional (ρ_s,η_s), octahedral (ρ_0,η_0), and tetrahedral (ρ_t,η_t) sites. For the hcp lattice, $z=0.5$ if $c/a\geq\sqrt{8/3}$, and $z=\frac{1}{2}[\frac{1}{3}+\frac{1}{4}(c/a)^2]^{1/2}$ if $c/a\leq\sqrt{8/3}$.

	ρ_s (Å)	η_s	ρ_0 (Å)	η_0	ρ_T (Å)	η_T
bcc, Fe ($a=2.866$ Å)	$\frac{\sqrt{3}}{4}a=1.241$	0.355	$\frac{2-\sqrt{3}}{4}a=0.192$	0.065	$\frac{\sqrt{5}-\sqrt{3}}{4}a=0.361$	0.109
fcc, Ni ($a=3.517$ Å)	$\frac{\sqrt{2}}{4}a=1.244$	0.290	$\frac{2-\sqrt{2}}{4}a=0.515$	0.122	$\frac{\sqrt{3}-\sqrt{2}}{4}a=0.280$	0.070
hcp, Co ($a=2.504$ Å, $c=1.625a$)	1.248	0.408	0.520	0.173	0.283	0.096
hcp, Gd ($a=3.631$ Å, $c=1.591a$)	1.785	0.402	0.761	0.173	0.420	0.098

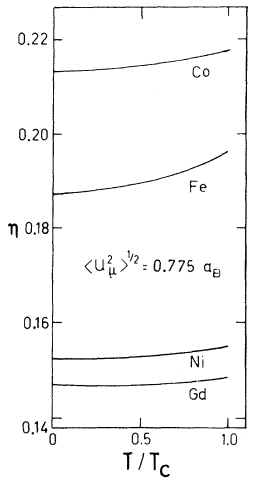

FIG. 4. Temperature dependence of η [see Eq. (16)] for Gd, Ni, Fe, and Co. The increase of lattice vibrations with temperature always dominates the lattice expansion, so that η is slightly increasing with T. The constant part of η is the temperature-independent zero-point motion of the muon with spatial extension $\langle u_\mu^2 \rangle^{1/2} = 0.775 a_B$.

consistent way. This demonstrates again that the effective screened electrostatic potential $V_\lambda(r)$ [Eq. (18)] is a very good approximation for calculations of electronic densities close to the muon.

The results of the model applied to Ni are given in Fig. 6 (octahedral site) and Fig. 7 (substitutional site). In the former case the spin density is negative for $\eta < 0.3$ and shows a much smaller dependence on η than in Gd.

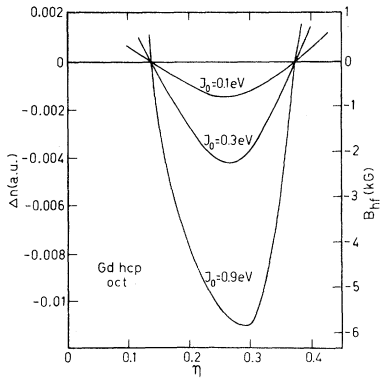

FIG. 5. Behavior of the spin density and hyperfine field as a function of the vibration parameter η for Gd for various values of the exchange interaction J_0. The muon is at the octahedral interstitial site. The theoretical estimate for J_0 is 0.83 eV, and η is expected to lie between 0.2 and 0.3. One can understand these curves with the help of the modified RKKY model (see Appendix).

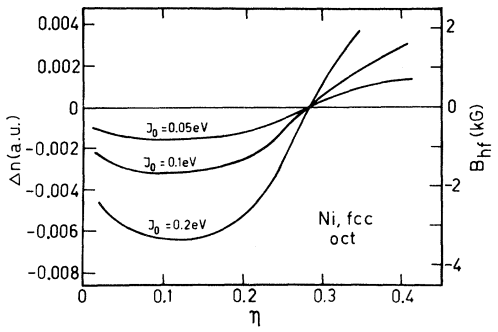

FIG. 6. Behavior of the spin density and hyperfine field at a muon at the octahedral interstitial site in Ni, as a function of the vibration parameter η. The dependence on η is much less pronounced than in the case of Gd. This can be understood within the modified RKKY model (see Appendix).

Several microscopic calculations have been proposed to explain the experimentally observed value of $B_{hf} = -0.71$ kG in Ni. From a cluster calculation[9] the value -0.59 kG was obtained. Using KKR methods, Katayama *et al.*[10] got -0.72 kG and with supercell band-structure methods, Jepsen *et al.*[12] predicted -0.463 kG. All these calculations assumed rigid positions of the ions and muon. An inspection of Fig. 7 shows that in the case of Ni the influence of the zero-point motion on the spin densities at the muon at the octahedral site is much smaller than for Gd, Dy, or Fe.[17] Thus Ni seems to be a good candidate for rigid microscopic theories. Calculations for Co and Fe (see Secs. V and VI) also show a strong dependence of B_{hf} on vibrations.

The general features of these results can be un-

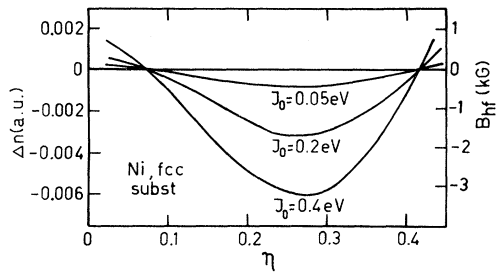

FIG. 7. In contrast to Fig. 6, when the muon is at a substitutional site in Ni, the dependence of B_{hf} on the vibration parameter η is very strong. The main difference from the octahedral interstitial case is a larger distance between the muon and the first shell (see Appendix).

derstood in the framework of the modified RKKY model described in the Appendix. The main conclusion of this discussion is that the sign of the hyperfine field and its dependence on vibrations depend crucially on the distance between the impurity and the first and second neighboring shells. Any change in this distance (e.g., lattice relaxation[19]) may act in a non-negligible way on the hyperfine field. Furthermore, the curves $B_{hf}(\eta)$ vary from one host to the other. Thus, the effect of the zero-point motion on the hyperfine field has to be calculated for every host separately.

V. DEPENDENCE ON TEMPERATURE

The temperature dependence of the hyperfine field $B_{hf}(T)$ at nonmagnetic impurities does not generally follow the host magnetization $M_s(T)$. This has also been observed for hyperfine fields at muons. The deviation $D(T)$ has been defined in Eq. (1):

$$D(T)=\frac{B_{hf}(T)}{B_{hf}(0)}-\frac{M_s(T)}{M_s(0)} .$$

The experiments give $D(T)<0$ for Gd, Fe, and Co but $D(T)>0$ for Ni for all temperatures (see Table I) from 0 to T_c. In the framework of our model, the temperature dependence of the lattice constant and of the mean-square elongation of the host atoms can easily be taken into account, as well as the decrease with increasing T of the effective exchange interaction J_T which follows the saturation magnetization $M_s(T)$.

As already mentioned, the parameter η is always slightly increasing with T (see Fig. 4). The increase of η leads to either a decrease or an increase of the magnitude of B_{hf}, depending on the value taken for $\eta_0=\eta(T=0)$. For instance, an inspection of Fig. 5 shows that in Gd, for $\eta_0\simeq 0.2$, $\partial B_{hf}/\partial\eta<0$, but for $\eta_0\simeq 0.3$ this derivative is greater than 0. These two choices correspond to different deviations $D(T)$ (see Table IV). In addition, B_{hf} changes when the lattice constant is increased. In the following, we present the results of the calculations for $T/T_c=0.3$, 0.6, and 0.9.

A. Gd

Table IV shows the measured ratios $M_s(T)/M_s(0)$ of the host magnetization, the μSR data $B_{hf}(T)/B_{hf}(0)$ and the results of the model calculations for the octahedral site. As mentioned above, we obtain a positive deviation $D(T)$ for $\eta_0\simeq 0.2$. For $\eta_0\simeq 0.3$, $D(T)$ is negative and the calculated values of $B_{hf}(T)/B_{hf}(0)$ are in rough agreement with the experiment.

B. Ni

In our model, the variation of B_{hf} with η at the octahedral site is rather small and the main effect on the temperature dependence of B_{hf} stems from the lattice expansion. This gives rise to a negative deviation (see Table V) which is in marked contrast to the experiments. However, a positive $D(T)$ is obtained for the substitutional site. It should be noticed that a curve similar to Fig. 7 could be obtained from the octahedral site if a positive lattice relaxation is included.

It may well be that the assumptions of the present model are invalid in the case of Ni. It should be mentioned that the calculations by Kanamori *et al.*,[11] based on first principles, explain not only the observed hyperfine field at absolute zero but also its temperature dependence,

TABLE IV. Temperature dependence of the normalized saturation magnetization compared to the observed and calculated temperature dependence of the normalized hyperfine field at a muon in Gd at the octahedral interstitial site. A negative deviation $D(T)$ [Eq. (1)] corresponding to the experimental result is obtained for a vibration parameter at 0 K of $\eta_0=0.3$. For $\eta_0=0.2$ a positive deviation is obtained, as expected from Fig. 5.

Gd		$B_{hf}(T)/B_{hf}(0)$		
T/T_c	$M_s(T)/M_s(0)$	Expt.	Oct., $\eta_0=0.2$	Oct., $\eta_0=0.3$
0.3	0.937	0.92	0.95	0.93
0.6	0.789	0.75	0.80	0.77
0.9	0.479	0.42	0.50	0.47

TABLE V. Temperature dependence of the normalized saturation magnetization compared to the temperature dependence of the normalized hyperfine field at a muon in Ni at the octahedral and substitutional sites for the same value of the vibration parameter at 0 K ($\eta_0=0.2$). The positive deviation $D(T)$ [Eq. (1)] obtained experimentally cannot be reproduced within the model at the octahedral site unless a positive lattice relaxation is included. At the substitutional site, however, the deviation is positive.

Ni		$B_{hf}(T)/B_{hf}(0)$		
T/T_c	$M_s(T)/M_s(0)$	Expt.	Oct., $\eta_0=0.2$	Subst., $\eta_0=0.2$
0.3	0.98	0.99	0.97	0.99
0.6	0.90	0.95	0.87	0.94
0.9	0.56	0.65	0.52	0.59

which is mainly dominated by single-particle excitations.

C. Fe

As in the case of Ni, we obtain $D(T)<0$ at the interstitial (tetrahedral) site, and $D(T)>0$ at the substitutional site (see Table VI). The result for the interstitial site agrees with the experiment. The calculations for the substitutional site will be discussed in the next section.

D. Co

The case of Co is particularly interesting because of the structural phase transition at 690 K where the host magnetization increases by about 2% while the amplitude of the hyperfine field at the muon decreases by some 5%. This behavior can be understood by an inspection of Fig. 8 which gives the dependence of the hyperfine field on vibrations in both phases. The phase transition corresponds to a jump from a full line to the corresponding dotted line which results in a net decrease of the magnitude of B_{hf}. The amplitude of the change $\Delta B_{hf}=B_{hf}(\text{hcp})-B_{hf}(\text{fcc})$ depends on the choice of η but ΔB_{hf} is clearly always negative.

By fixing the model parameters J_0 and η_0, we have calculated the spin density at the octahedral site in both lattices, taking into account the change in the lattice constant and the increase of M_s. The result for $J_0=0.3$ eV and $\eta_0=0.2$ is shown in Fig. 9. Furthermore, $D(T)$ is negative as expected from Fig. 8.

VI. DEPENDENCE ON VOLUME AND SITE

Butz *et al.*[34] have measured the local magnetic field at muons in Fe and Ni at room temperature as a function of applied hydrostatic pressure up to 7 kbar. Using the known dependence of magnetization and volume on pressure, the change of B_{hf} with volume could be determined. In the framework of our model, we have calculated the change in the spin density with the lattice constant keeping $J_0=0.2$ eV and $\eta=0.2$ fixed.

For the muon at the tetrahedral site in Fe (at the octahedral site in Ni), we obtained for Fe (Ni)

$$\frac{\partial \ln B_{hf}}{\partial \ln a}=1.5\ \ (0.3)\ . \tag{21}$$

TABLE VI. Temperature dependence of the normalized saturation magnetization compared to that of the normalized hyperfine field at a muon in Fe at the tetrahedral (substitutional) site, with vibration parameter $\eta_0=0.2$ ($\eta_0=0.3$).

Fe		$B_{hf}(T)/B_{hf}(0)$		
T/T_c	$M_s(T)/M_s(0)$	Expt.	Tetr., $\eta_0=0.2$	Subst., $\eta_0=0.3$
0.3	0.98	0.97	0.95	0.99
0.6	0.90	0.87	0.84	0.93
0.9	0.61	0.54	0.51	0.64

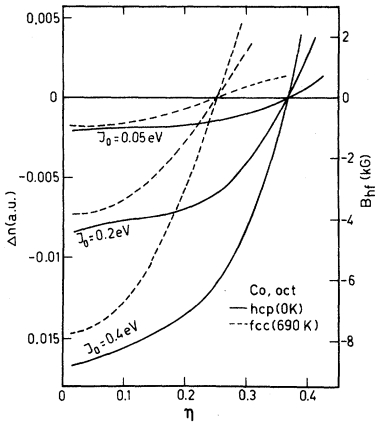

FIG. 8. Behavior of the spin density and hyperfine field at a muon at the octahedral interstitial site in Co for both the fcc and hcp phases with the same values of the exchange interaction J_0.

A change in the volume will also change the mean-square elongations. This can only be accounted for by calculations of the potential. If it is assumed that $\langle u^2 \rangle$ is proportional to a^2, the value of η remains unchanged. Assuming, furthermore, that the hyperfine field is proportional to the magnetization, we get

$$\frac{\partial \ln B_{\rm hf}}{\partial \ln V} = \frac{1}{3} \frac{\partial \ln B_{\rm hf}}{\partial \ln a}\bigg|_{M=\text{const}} + \frac{\partial \ln M}{\partial \ln V} . \quad (22)$$

With the value 0.47 (0.37) for $\partial \ln M / \partial \ln V$ for Fe (Ni), we thus obtain

$$\frac{\partial \ln B_{\rm hf}}{\partial \ln V} = 0.97 \ \ (0.47) .$$

The experimental values are 0.92 for Fe and 2.7 for Ni. The Fe value agrees satisfactorily with the experiment, but the model completely fails to explain the Ni result.

Very recently it was possible[35] to observe a previously unobserved μSR signal in a Fe crystal which had been irradiated with electrons. From the annealing characteristics, the signal could be identified as stemming from muons at monovacancies. It is therefore of some interest to discuss in some detail the predictions of the present model concerning the dependence on the muon site. A quantitative discussion is, of course, not possible since the zero-point motion of the muon is site dependent, and the hyperfine fields calculated for Fe strongly depend on η, as can be seen in Fig. 10.

Qualitatively, however, the following conclusions can be drawn: At an interstitial site, η is expected to be smaller than 0.2. If $\eta_{\rm subst} \simeq \eta_{\rm tetr}$, $|B_{\rm hf}(\text{subst})|$ is expected to be some 20% smaller than $|B_{\rm hf}(\text{tetr})|$. On the other hand, if $\eta_{\rm subst} \simeq 2\eta_{\rm tetr}$, the reduction is about 50%. Adjusting the effective interaction J_0 such that the hyperfine field at the tetrahedral site agrees with the experimental value of -11.1 kG, we expect a value between -6 and -9 kG for $B_{\rm hf}$(subst). This differs from the results of Kanamori *et al.*[11] who predicted $B_{\rm hf}(\text{subst}) = +0.32$ kG.

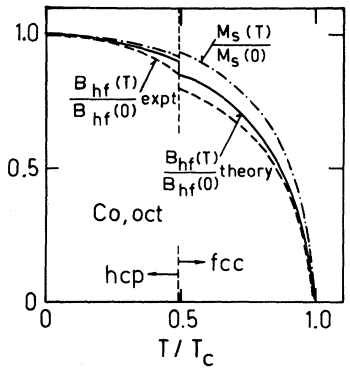

FIG. 9. Temperature dependence of the normalized saturation magnetization and the experimental and calculated normalized hyperfine fields at a muon at the octahedral site in Co (for $J_0=0.3$ eV and $\eta_0=0.2$). Although M_s increases at the phase transition ($T=690$ K) by about 2%, the magnitude of the calculated $B_{\rm hf}$ decreases by some 5%, which is also observed experimentally.

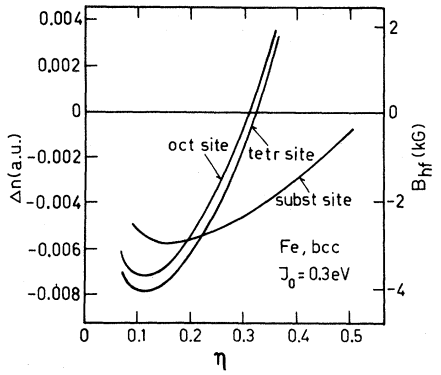

FIG. 10. The dependence of the hyperfine field and the spin density on the vibration parameter η in Fe, with a muon at the octahedral, tetrahedral, or substitutional sites calculated with the exchange interaction $J_0=0.3$ eV. At the substitutional site the muon sees a negative hyperfine field of smaller amplitude than at an interstitial site.

The experiments done so far have not permitted a determination of sign of the total local field at the muon at this site, so that the value of the hyperfine field is[35] either -5.2 or -9.6 kG. A less questionable prediction of the model concerns the temperature dependence of the hyperfine field at the substitutional site. Owing to the much less pronounced variation of the spin density at the substitutional site, the deviation introduced in Eq. (1) is positive (see Table VI), in contrast to the negative value calculated for the tetrahedral site. This seems to be in agreement with recent experiments.[35]

For Ni, the first-principles calculations of Kanamori[10,11] predict a muon hyperfine field at a substitutional site of 4.25 kG which is analogous to the case of boron. Our model also gives a positive value for the rigid case ($\eta=0$) but a negative value if the zero-point motion is accounted for. Experiments on Ni with vacancies would be very interesting.

VII. CONCLUSIONS

A model was developed which describes the hyperfine fields at nonmagnetic impurities in ferromagnetic metals. The model was applied to study the spin density at muons in Gd, Dy, Ni, Fe, and Co. In most lattices, the spin density depends crucially on the zero-point motion of the muon. The influence of vibrations on the hyperfine field was discussed in a modified RKKY-type model. This allows one to understand the numerical results obtained from the full model. The temperature dependence of $B_{\rm hf}$ was calculated, taking into account lattice expansion and thermal vibration of the lattice ions. Agreement with the experiment was found except for the case of Ni. This failure is tentatively interpreted as being due to the neglect of the unknown lattice relaxation around the μ^+ since, in Ni, the hyperfine field at the octahedral interstitial site depends strongly on the distance to the first- and second-nearest neighbors. The calculated pressure dependence agrees well with the data for Fe, but disagrees again for Ni. Further, the model predicts changes in $B_{\rm hf}$ and its temperature dependence for the substitutional site.

Since the model is based on a localized exchange interaction between itinerant electrons and localized moments as are the approaches in Refs. 4, 5, or 19, it is too crude to give reliable absolute numbers for $B_{\rm hf}$. Its merit, however, lies in the possibility of investigating relative changes and studying geometrical effects. This is best documented by the change in $B_{\rm hf}$ at the structural phase transition in Co. Other models[7,36] emphasize different mechanisms for the origin of hyperfine fields. Microscopic treatments,[8–12] on the other hand, usually leave out certain physical effects for technical reasons. Quantitative theoretical results for hyperfine fields at light impurities would not only require a microscopic theory for the exchange mechanism, but also a calculation of the lattice potential which accounts for the large zero-point motion of the muon.

APPENDIX: RKKY MODEL WITH VIBRATIONS

It is interesting to investigate the influence of vibrations on the spin density induced by a single magnetic ion. This gives some insight into the results obtained by the numerical solutions of the model discussed in Sec. IV.

A fixed magnetic moment induces an oscillating spin density in a homogeneous electron gas, which then leads to an effective coupling between two localized moments. Neglecting the electrostatic potential of the muon, the enhancement factor is given in linear approximation by[16]

$$E_\sigma(k)=1-\frac{2}{k}\int_0^\infty dr\, W_\sigma(r)\sin(2kr)\ . \tag{A1}$$

The relative spin density is then calculated from (20):

$$\frac{\Delta n(0)}{n_0}=-6\int_0^\infty dr\, rf(2k_Fr)[W_+(r)-W_-(r)]\ , \tag{A2}$$

where

$$f(y)=\frac{\sin y}{y^3}-\frac{\cos y}{y^2}\ . \tag{A3}$$

For the potential produced by a fixed ($\eta=0$) localized moment

$$W_\sigma(r)=-\sigma J_T\Omega\frac{\delta(r-R)}{4\pi R^2}\ , \tag{A4}$$

we obtain the familiar RKKY result

$$\frac{\Delta n(0)}{n_0}=3J_T\Omega\frac{f(2k_FR)}{\pi R}\ . \tag{A5}$$

The effect of charge screening can easily be incorporated. In the distorted-wave Born approximation, one obtains[16]

$$\frac{\Delta n(0)}{n_0}=\frac{3J_T\Omega}{2\pi k_F^3 R^2}\int_0^{k_F} dk\, kE_\lambda(k)\sin(2kR) \tag{A6}$$

which reduces to (A5) for $E_\lambda(k)\equiv 1$.

Using the known[24] enhancement factor $E_\lambda(k)$ for $V_\lambda(r)$ [see Eq. (18)], the enhanced spin density can be calculated. The results are shown in Fig. 11, together with the function $yf(y)$ characterizing the RKKY result. The inclusion of charge screening leads to a large enhancement of the oscillations as well as to a shift in the phase. The qualitative picture, however, remains unchanged. Introducing the averaged potential of Sec. II, we obtain for a single vibrating lattice ion (with η' standing for $2k_F a\eta$):

$$W_\sigma(r)=\frac{\sigma J_T\Omega}{4\pi^{3/2}\eta' rR}e^{-(r-R)^2/\eta'^2}. \tag{A7}$$

The spin density is determined from

$$\frac{\Delta n(0)}{n_0}=\frac{3J_T\Omega}{\pi^{1/2}R}\int_0^{\infty} dx\, e^{-x^2} f(2k_F(R+\eta' x)). \tag{A8}$$

For small values of η', the integrand can be expanded and we obtain

$$\frac{\Delta n(0)}{n_0}=\frac{3J_T\Omega}{\pi R}[f(2k_F R)+\eta'^2 k_F^2 f''(2k_F R)+\cdots]. \tag{A9}$$

One sees that for small η' the spin density depends quadratically on the vibrations of the impurity and of the lattice ions with a curvature that is positive or negative depending on the sign of the second derivative f'' at $y=2k_F R$.

The dependence of the spin density on η' as given by Eq. (A8) is shown in Fig. 12 for various values of y. It is evident that the sign of the spin density and its dependence on vibrations depend crucially on the value of $y=2k_F R$, i.e., mainly on the distance between the muon and the magnetic ion. This result can be used to discuss the curves obtained for Gd and Ni using the full model (see Sec. IV).

The strong dependence of the spin density on η for Gd (Fig. 5) can be interpreted as follows: For $\eta=0$ we get a positive spin density as is the case for a single magnetic ion at a distance $y_1=2k_F R_1\simeq 8$ (see Fig. 11) corresponding to the

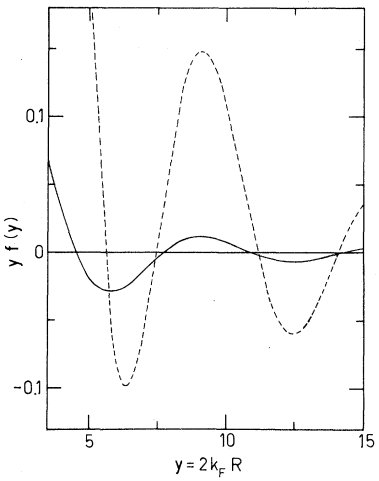

FIG. 11. The function $f(y)$ [Eq. (A3)] is proportional to the spin density induced by a single magnetic ion in the RKKY model when no vibrations are present. $y=2k_F R$ measures the distance from the fixed localized magnetic moment. The dotted curve is the same function of the spin density when the charge screening potential $V_\lambda(r)$ [Eq. (18), with $\lambda=1.3$] is taken into account. Depending on the value of y, the spin density can be positive or negative, with a positive or negative curvature $f''(y)$.

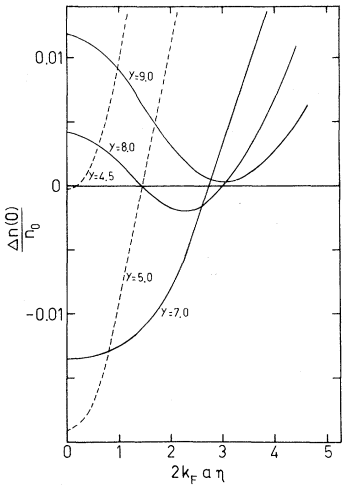

FIG. 12. Spin density produced by a single magnetic ion as a function of the vibrations η, in the modified RKKY model for various values of $y=2k_F R$, where R is the distance between the muon and the localized magnetic moment. The dependence of the hyperfine field on the vibrations depends crucially on R (see Fig. 11), i.e., on the lattice constant, lattice relaxation, or any change in the distance between the muon and its nearest neighbor.

nearest-neighbor distance from the octahedral site for Gd. With increasing η, the contribution of the negative amplitude for $y < 7.5$ first dominates and keeps the average field negative until the vibration is so large that the positive amplitude for $y < 5$ gives the main contribution. In the case of a muon at the octahedral site in Ni (Fig. 6), the spin density shows a much less pronounced dependence on η. We attribute this behavior to the partial cancellation of the negative contribution from the six nearest neighbors ($2k_F R_1 = 5.56$) and the positive contribution from the eight next-nearest neighbors ($2k_F R_2 = 9.63$) (see Fig. 11). For the substitutional site (Fig. 7), there are twelve nearest neighbors ($2k_F R_1 = 9.63$) with a positive field for $\eta = 0$. The same kind of arguments help to understand the curve obtained for Co (Fig. 8) and Fe (Fig. 10).

ACKNOWLEDGMENTS

It is a pleasure to thank A. B. Denison and M. Manninen for constructive discussions and W. Kündig, B. D. Patterson, and K. Petzinger for critical reading of the manuscript. This work has been partially supported by the Swiss National Science Foundation.

[1]For a comprehensive review of the μSR work on ferromagnetic materials, see A. B. Denison, H. Graf, W. Kündig, and P. F. Meier, Helv. Phys. Acta 52, 460 (1979).

[2]For a tutorial article see P. F. Meier, in *Exotic Atoms 79*, edited by K. M. Crowe, J. Duclos, G. Fiorentini, and G. Torelli (Plenum, New York, 1979).

[3]P. F. Meier, W. Kündig, B. D. Patterson, and K. Rüegg, Hyperfine Interact. 5, 311 (1978).

[4]E. Daniel and J. Friedel, J. Phys. Chem. Solids 24, 1601 (1963).

[5]A. Blandin and I. A. Campbell, Phys. Rev. Lett. 31, 51 (1973).

[6]P. Jena and D. J. W. Geldart, J. Magn. Magn. Mater. 8, 99 (1978).

[7]M. B. Stearns, Phys. Rev. B 13, 4180 (1976); M. B. Stearns and J. M. Norbeck, *ibid.* 20, 3739 (1979).

[8]K. Petzinger and R. Munjal, Phys. Rev. B 15, 1560 (1977).

[9]J. Keller and B. D. Patterson, Hyperfine Interact. 6, 73 (1979).

[10]H. Katayama, K. Terakura, and J. Kanamori, Solid State Commun. 29, 431 (1979).

[11]J. Kanamori, H. K. Yoshida, and K. Terakura, Hyperfine Interact. 8, 573 (1981).

[12]O. Jepsen, R. M. Nieminen, and J. Madsen, Solid State Commun. 34, 575 (1980).

[13]P. Jena, Hyperfine Interact. 6, 5 (1979), and references quoted therein.

[14]P. F. Meier, W. Kündig, and K. Rüegg, Hyperfine Interact. 6, 77 (1979).

[15]P. F. Meier, Solid State Commun. 27, 1163 (1978).

[16]P. F. Meier, and A. B. Denison, J. Appl. Phys. 50, 7548 (1979).

[17]S. Estreicher, A. B. Denison, and P. F. Meier, Hyperfine Interact. 8, 601 (1981).

[18]M. Manninen and P. Jena, Phys. Rev. B 22, 2411 (1980).

[19]M. Manninen and R. M. Nieminen, J. Phys. F 11, 1213 (1981).

[20]P. Jena, Phys. Rev. Lett. 36, 418 (1976).

[21]K. Nishiyama, F. Dimmling, T. Kornrumpf, and D. Riegel, Phys. Rev. Lett. 37, 357 (1976).

[22]C. O. Almbladh and U. von Barth, Phys. Rev. B 13, 3307 (1976).

[23]P. F. Meier, Hyperfine Interact. 6, 29 (1979).

[24]P. F. Meier, Helv. Phys. Acta 48, 227 (1975).

[25]R. M. Moon, W. C. Koehler, J. W. Cable, and H. R. Child, Phys. Rev. B 5, 997 (1972).

[26]H. A. Mook and C. G. Shull, J. Appl. Phys. 37, 1034 (1960).

[27]C. G. Shull and H. A. Mook, Phys. Rev. Lett. 16, 184 (1966).

[28]R. M. Moon, Phys. Rev. A 136, 195 (1964).

[29]H. Teichler, Hyperfine Interact. 6, 251 (1979).

[30]J. Rath, M. Manninen, P. Jena, and C. S. Wang, Solid State Commun. 31, 1003 (1979).

[31]V. Hovi and M. Komu, Ann. Acad. Sci. Fenn. A VI, No. 412 (1974).

[32]F. E. Obenshain and H. H. F. Wegener, Phys. Rev. 121, 1344 (1961).

[33]T. A. Kovats and J. C. Walter, Phys. Rev. 181, 610 (1969).

[34]T. Butz, J. Chappert, J. F. Dufresne, O. Hartmann, E. Karlsson, B. Lindgren, L. O. Norlin, P. Podini, and A. Yaouanc, Phys. Lett. 75A, 321 (1980).

[35]H. Graf (private communication).

[36]M. B. Stearns, Hyperfine Interact. 8, 583 (1981).